Available online at www.sciencedirect.com

ScienceDirect

Energy Procedia 55 (2014) 128 – 132

Energy Procedia

4th International Conference on Silicon Photovoltaics, SiliconPV 2014

Analysis of the impact of doping levels on performance of back contact - back junction solar cells

Paul Procel[a], Vincenzo Maccaronio[a], Felice Crupi[a], Giuseppe Cocorullo[a], Mauro Zanuccoli[b], Paolo Magnone[b], Claudio Fiegna[b]

[a]*DIMES, University of Calabria, Via P. Bucci c/o Cubo 42/C, I-87036,Rende (CS), Italy*
[b]*ARCES-DEI, University of Bologna, Via Venezia 260, I-47521 Cesena (FC), Italy*

Abstract

In this work, by exploiting two-dimensional (2-D) TCAD numerical simulations, we performed a study of the impact of the doping levels on the main figures of merit in the different regions of a crystalline silicon Back-Contact Back-Junction (BC-BJ) solar cell: the emitter, the Back Surface Field (BSF) and the Front Surface Field (FSF). The study is supported by a dark loss analysis which can highlight the contribution of several recombination mechanisms to the total diode saturation current. The efficiency curve as a function of doping level exhibits a bell-shape with a clearly identifiable optimum value for the three regions. The decrease in efficiency observed at lower doping values is explained in terms of higher contact recombination for BSF and emitter, and in terms of higher surface recombination for FSF. The efficiency decrease observed at higher doping values is ascribed to the higher surface recombination for FSF and Auger recombination for all cases.

Peer-review under responsibility of the scientific committee of the SiliconPV 2014 conference

Keywords: BC-BJ solar cell; TCAD simulation; dark analysis; doping peak

1. Introduction

Silicon-based Back-Contact Back Junction solar cells (BC-BJ) have been demonstrated particularly promising in order to improve the conversion efficiency because of their architecture with no shadowing areas and simplification of cell interconnection on the rear side. Moreover, efficiencies over 24% have been already reported [1] with the potential to go beyond.

Several works have been developed to study the optimization of BC-BJ in geometry and doping characteristics [2] [3] reporting efficiency trends by changing geometrical parameters. In this work, by exploiting TCAD simulations, we analyse the performance trend of BC-BJ changing the doping peak concentration of emitter, Back

Peer-review under responsibility of the scientific committee of the SiliconPV 2014 conference
doi:10.1016/j.egypro.2014.08.095

Surface Field (BSF), Front Surface Field (FSF), in terms of recombination losses. In this way, every analysis was developed by performing two simulations: the cell under illumination and under dark conditions to define the recombination losses [4] by extracting Shockley-Read-Hall (SRH), Auger, Surface and contact contributions to the total recombination current and relate them to the efficiency trend.

From this work emerges that, within the range of geometrical and physical parameters considered in our study, the physics of each region is independent from the others and there is a trade-off between two different recombination mechanisms that leads to one optimum intermediate doping peak value for each region.

2. Simulation methodology

Fig.1. shows the sketch of the symmetry element of the simulated solar cells. In this work we considered a floating-zone (FZ-Si) n-type doped 200µm-thick silicon wafer featuring resistivity 2 Ω-cm. The doping profiles in BSF, FSF and emitter are Gaussian functions of the spatial coordinate featuring the peak located at the edge of the interface and junction depth of 2µm for BSF and Emitter and of 1µm for FSF region.

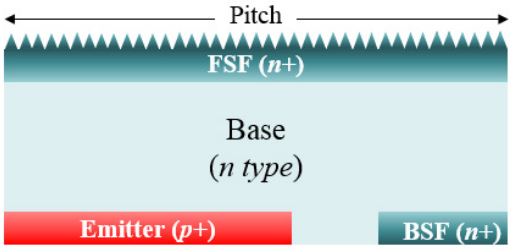

Fig.1. Sketch of the symmetry element of BC-BJ solar cell used in the simulations. Pitch =955µm, Gap=5µm

We assumed as simulation parameters the peak doping concentration of the emitter ($C_{em,pk}$), the BSF ($C_{bsf,pk}$) and the FSF ($C_{fsf,pk}$) regions. The front surface is coated by double-layer Anti-Reflective Coating (ARC) composed by 42nm Si_3N_4 and 27nm SiO_2, texturized by regular upright pyramids featuring a 10 µm base, while the back side is passivated by a 0.1 µm of SiO_2.

In order to predict realistic values of the figures of merit, the physical models have been calibrated by means of state-of-the-art parameterizations [5]. Fermi–Dirac statistics is adopted to correctly deal with large doping concentrations. The Bandgap narrowing model (BGN) proposed by Schenk is used to account for commonly adopted values of intrinsic carrier density in photovoltaic community (n_i=9.65x10^{-9} cm^{-3} at T=300 K) [6]. The model proposed by Klaassen in [7] has been adopted in order to model the doping dependent carrier mobility. Auger and radiative recombination models have been parameterized according to Richter *et al* in [8]. Recombination losses due to trap-assisted recombination is modelled by assuming the single-level trap model by Shockley–Read–Hall (SRH); the doping-dependent carrier lifetimes in phosphorus-doped FZ-Si are calculated according to [9]. Surface Recombination Velocity at passivated interfaces has been modelled according to semi empirical models proposed by Altermatt in [10]. The surface velocity at electrodes is set to 1x10^6 cm/s.

The solar cell has been simulated changing one peak doping concentration in each analysis and assuming the others doping levels constant at optimum values. The study has been performed at T=298K under illumination, with a standard AM1.5G spectrum (1000 W/m^2) [11], and in dark conditions to calculate the impact of the recombination losses on the main figures of merit.

3. Results and discussion

In order to understand the impact of doping peak profile on the main figures of merit, we have performed an extensive set of numerical simulations by using the state-of-the-art finite element simulator Sentaurus TCAD [3].

We assumed as simulation parameters the peak concentrations of the emitter doping, of the BSF doping and of the FSF doping. In the following, we discuss separately each analysis.

3.1. Emitter doping analysis

As it can been seen in Fig. 2 (a), remarkable variations of V_{oc}, FF and consequently of conversion efficiency (η) occur with increasing peak doping concentration of the emitter diffusion ($C_{em,pk}$). It is worth noting that the short-circuit current density J_{sc} has a negligible dependence on the peak doping concentration in the emitter region. Indeed, the effects of the doping variation occur in a relatively small region in the rear side of the cell where the carrier photogeneration is the lowest. On the other hand, the FF increases with increasing $C_{em,pk}$ due to a reduction of the emitter sheet resistance. A trade-off between two competitive mechanisms leads to an optimum $C_{em,pk}$ value (at approximately $1.2x10^{19}$ cm^{-3}) which allows the maximization of the V_{oc}: minority carrier density at contact interface and Auger recombination loss. At first, an increase in doping concentration in emitter region leads to an increase of V_{oc} due to a greater depletion region. However, the decrease in V_{oc} above $C_{em,pk}$ equal to $1.2x10^{19}$ cm^{-3} is observed; the degradation of V_{oc} is explained by the trend of the saturation current density calculated under dark conditions illustrated in Fig 2 (b). For relatively low emitter doping concentration peaks, the recombination at contacts is the main component of the total recombination, due to a decrease of minority carriers on emitter region caused by a stronger electrical field on the junction; this explains why the SRH and the Surface Recombination exhibit a negligible dependence on $C_{em,pk}$. However, for peak doping level above $1.2x10^{19}cm^{-3}$, Auger recombination becomes stronger and predominant on the total recombination as we expected in the case of doping profiles exhibiting higher peak concentration. Therefore, a trade-off between electrical field intensity in the junction and Auger recombination rate is observed.

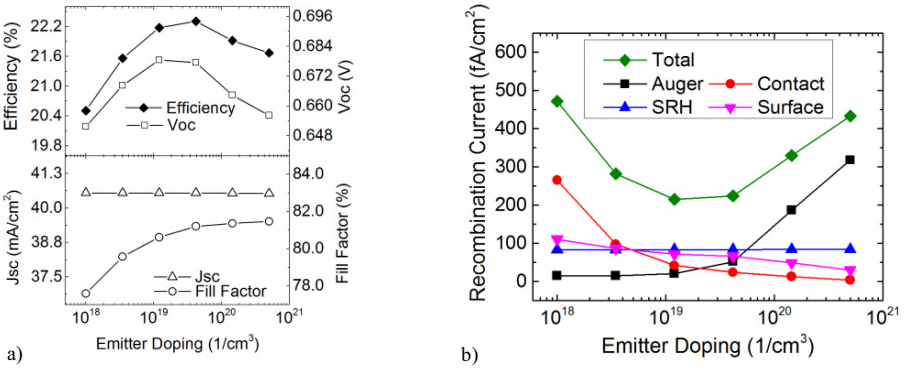

Fig.2. a) Efficiency, open-circuit voltage V_{oc}, short-circuit current density J_{sc} and Fill Factor for Emitter doping $C_{em,pk.}$ b) Dark recombination current density components for simulations changing Emitter doping $C_{em,pk.}$

3.2. BSF doping analysis

The change in peak doping concentration on BSF ($C_{bsf,pk}$) has a significant impact on J_{sc} as shown in Fig 3 (a). We observe an increasing trend of J_{sc} with increasing $C_{bsf,pk}$ due to the enhanced effectiveness of the electrical field distribution which prevents minority carrier recombination at the rear contact. In addition, this leads to an increase in Voc. However, as it can be seen in Fig. 3 (b) Auger recombination becomes important for BSF doping peaks above approximately $1.44x10^{20}cm^{-3}$. On the contrary, a negligible influence of $C_{bsf,pk}$ on SRH and Surface recombination contributions to the total saturation current density is observed. This is ascribed to the increase in either carrier doping-dependent lifetime and surface recombination velocity at the Si/SiO2 interface with increasing $C_{bsf,pk}$ which is compensated by a reduction of the amount of the excess of minority carriers thanks to the relatively

stronger electrical field. The trend of the total recombination current is in agreement to those of J_{sc} and V_{oc}; in conclusion an optimum value of $C_{bsf,pk}$ ($1.44x10^{20}cm^{-3}$) can be calculated.

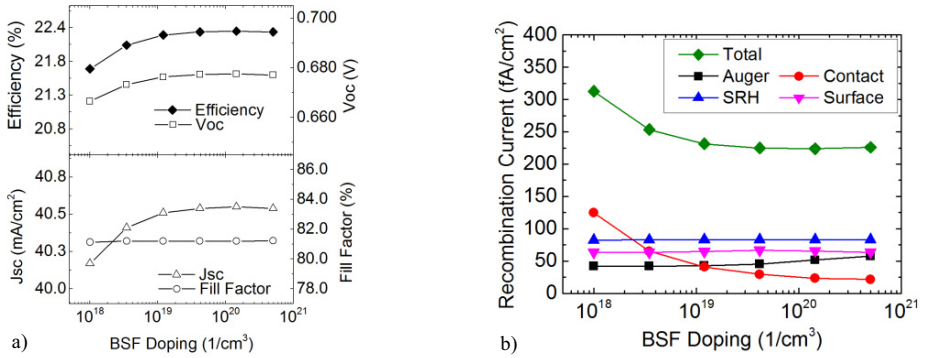

Fig.3. a) Efficiency, open-circuit voltage V_{oc}, short-circuit current density J_{sc} and Fill Factor for BSF doping $C_{bsf,pk}$. b) Dark recombination current density components for simulations changing BSF doping $C_{bsf,pk}$.

3.3. FSF doping analysis

Similarly to the case of the BSF doping analysis, changes in FSF doping peak ($C_{fsf,pk}$) influence markedly the main figures of merit, in particular the J_{sc}, as Fig. 4 (a) shows. According to the dark analysis illustrated in Fig. 4 (b), we observe a decrease in the contribution to the total saturation current density due to the surface recombination at the Si/SiO_2 interface with increasing $C_{fsf,pk}$. Indeed, higher doping peaks lead to relatively more intense electrical field reducing consequently the minority carriers concentration overall in the FSF region. However, for higher $C_{fsf,pk}$ values, the Auger recombination contribution and surface recombination velocity increase enough to become significant.

According to our simulations, the inflection point of the FSF doping is $3.47x10^{18}cm^{-3}$. It is worth noting that the increase in SRH and surface recombination current density is marked above $3.47x10^{18}$ cm^{-3} thanks to the dependence of lifetime and surface recombination velocity on doping concentration.

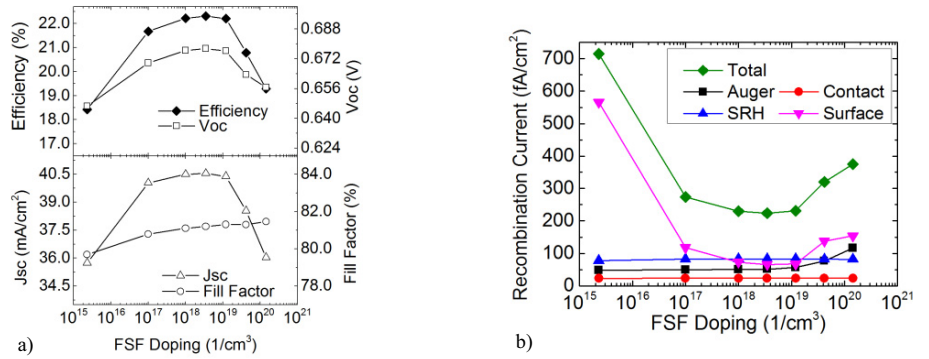

Fig.4. a) Efficiency, open-circuit voltage V_{oc}, short-circuit current density J_{sc} and Fill Factor for FSF doping $C_{fsf,pk}$. b) Dark recombination current density components for simulations changing FSF doping $C_{fsf,pk}$.

4. Conclusions

In this theoretical work we have carried out an extensive study of the impact of BSF, FSF and emitter doping profiles on the efficiency of the solar cell back-contact back-junction. The efficiency curve as a function of doping exhibits a bell shape with a clearly identifiable optimum value for the three doping regions. In our simulated structure, the optimum values of peak doping are: $4.16x10^{19}$ cm^{-3} for emitter, $1.44x10^{20}$ cm^{-3} for BSF and $3.47x10^{18}$ cm^{-3} for FSF. The efficiency decrease observed at lower doping values is explained in terms of higher contact recombination for BSF and emitter, and in terms of higher surface recombination for FSF. The efficiency decrease observed at higher doping values is explained in terms of higher Auger recombination for BSF and emitter, and in terms of higher surface and Auger recombination for FSF. Therefore, the optimum doping peak value is result of the trade-off between surface recombination at silicon interfaces and Auger recombination losses. This means that is expected that the optimum peak doping should change depending on the quality of the passivation at interfaces Si/SiO_2 and Si/Al.

References

[1] P. J. Cousins, David D. Smith, Hsin-Chiao Luan, Jane Manning, Tim D. Dennis, Ann Waldhauer, Karen E. Wilson, Gabriel Harley, William P. Mulligan., “Generation 3: Improved performance at lower cost”, Proc. 35th IEEE Photovoltaic Specialist Conference PVSC, Honolulu, Hawaii, USA, 2010, pp. 275-278

[2] J. Renshaw, A. Rohatgi. “Device optimization for screen printed interdigitated back contact solar cells”, Photovoltaic Specialists Conference (PVSC), 2011 37th IEEE

[3] D. S. Kim , V. Meemongkolkiat, A. Ebong, B. Rounsaville, V. Upadhyaya, A. Das and A. Rohatgi, “2D-Modeling and development of interdigitated back contact solar cells on low-cost substrates”, Photovoltaic Energy Conversion, Conference Record of the 2006 IEEE 4th World Conference on (Volume:2), May 2006. Pp 1417-1420

[4] P. Magnone, D. Tonini, R. De Rose, M. Frei, F. Crupi, E. Sangiorgi, C. Fiegna, “Numerical simulation and modeling of resistive and recombination losses in MWT solar cells” IEEE Journal of Photovoltaics, vol.3, no.4, pp.1215-1221, Oct. 2013

[5] Synopsis, “Sentaurus device user guide,” Version G-2012.06, June 2012.

[6] R. De Rose, M. Zanuccoli, P. Magnone, M. Frei, E. Sangiorgi, and C. Fiegna, "Understanding the impact of the doping profiles on selective emitter solar cell by two-dimensional numerical simulation,", IEEE Journal of Photovoltaics, vol.3, no.1, pp.159,167, Jan. 2013

[7] D. Klaassen, "A unified mobility model for device simulation: II. temperature dependence of carrier mobility and lifetime," Solid-State Electronics, vol. 35, no. 7, pp. 961-967, 1992.

[8] A. Richter, S. W. Glunz, F. Werner, J. Schmidt, A. Cuevas “Improved quantitative description of Auger recombination in crystalline silicon”, PHYSICAL REVIEW B 86, 165202 (2012).

[9] C. Reichel, F. Granek, M. Hermle, S. W. Glunz, “Investigation of electrical shading effects in back-contacted back-junction silicon solar cells using the two-dimensional charge collection probability and the reciprocity theorem”, J. Appl. Phys. 109, 024507, 2011.

[10] Pietro P. Altermatt, Jürgen O. Schumacher, Andres Cuevas, Mark J. Kerr, Stefan W. Glunz *et al* “Numerical modeling of highly doped Si:P emitters based on Fermi–Dirac statistics and self-consistent material parameters” J. Appl. Phys. **92**, 3187, 2002.

[11] ASTM G173-03 Tables: Extraterrestrial Spectrum, Terrestrial Global 37 deg South Facing Tilt & Direct Normal Circumsolar.